

Contents lists available at ScienceDirect

## Organic Geochemistry

journal homepage: www.elsevier.com/locate/orggeochem



## Extended chain length alkenoates differentiate three Isochrysidales groups



Sian Liao a,b, Karen J. Wang b,c, Yongsong Huang c,\*

- <sup>a</sup> Department of Chemistry, Brown University, 324 Brook Street, Providence, RI 02912, USA
- <sup>b</sup> Institute at Brown for Environment and Society, Brown University, Providence, RI 02912, USA
- <sup>c</sup> Department of Earth, Environmental and Planetary Sciences, Brown University, 324 Brook Street, Providence, RI 02912, USA

#### ARTICLE INFO

#### Associate Editor-Elizabeth Minor

Keywords:  $C_{37}OEt$  and  $C_{38}OEt$  alkenoates Alkenones: Group-specific biomarkers Isochrysidales Chemotaxonomy

#### ABSTRACT

Alkenoates and alkenones are polyunsaturated long-chain esters and ketones produced by members of the Isochrysidales, an order of haptophyte microalgae. Based on phylogenetic data, members of Isochrysidales have been classified into three groups, with each group showing major differences in preferred growth environments (e.g., salinity). Systematic identification of chemotaxonomic differences among the three groups of Isochrysidales is thus important for paleoenvironmental reconstructions and disentangling mixed alkenone temperature signals. Here, we systematically examined alkenone/alkenoate profiles in culture samples of Group 2 and Group 3 Isochrysidales and environmental sample of Group1 Isochrysidales. Using GC columns with stationary phases of contrasting polarities, we discovered for the first time  $C_{37}$  and  $C_{38}$  ethyl alkenoates ( $C_{37}$ OEt and  $C_{38}$ OEt) in Group 2 and/or 3 Isochrysidales, extending the longest alkenoate chain length of  $C_{36}$ OEt in previous publications. We show that Group 3 Isochrysidales only produce  $C_{37}$ OEt, whereas Group 2 Isochrysidales produce both  $C_{37}$ OEt and  $C_{38}$ OEt alkenoates. Because Group 1 Isochrysidales do not produce alkenoates,  $C_{38}$ OEt are specific biomarkers for Group 2 species. The identification of  $C_{37}$ OEt and  $C_{38}$ OEt in sediments from saline lakes and Chesapeake Bay where sequences of Group 2 DNA have been recovered further validates the use of  $C_{38}$ OEt as a Group 2-specific biomarker.

### 1. Introduction

Alkenoates and alkenones are polyunsaturated long-chain esters and ketones produced by the Isochrysidales, an order of haptophyte microalgae. For nearly 40 years, unsaturation ratios  $(U_{37}^{K})$  of alkenones have been widely used for paleo-sea surface temperature (SST) reconstructions (e.g., Brassell et al., 1986; Rosell-Melé and Comes, 1999; Tzanova and Herbert, 2015).

Based on 18S rRNA sequencing data, the Isochrysidales has been divided into three distinct phylogenetic groups, with each group showing major differences in preferred growth environments (Theroux et al., 2010): Group 1 in freshwater and oligohaline environments (Longo et al., 2018), Group 2 in saline lakes (Theroux et al., 2010, 2020; Randlett et al., 2014; Araie et al., 2018) and marginal ocean environments (Kaiser et al., 2019), and Group 3 in open ocean areas (Müller et al., 1998; Zheng et al., 2019). The preference of the three Isochrysidales groups for different salinity is well illustrated in the Baltic Sea whose salinity stretches from near 0 to 35 ppt over ~ 2000 km, with Group 1 found in the surface sediments of the freshest waters, Group 3

near open ocean and Group 2 in between (Kaiser et al., 2019). It is therefore possible to assess past salinity changes based on changes in Isochrysidales assemblages, as illustrated recently in salinity reconstructions in Black Sea for the past 16,000 years (Huang et al., 2021) and Lake Sayram for the past 3000 years (Yao et al., 2020).

Identification of mixed alkenone productions in ocean (Kaiser et al., 2019; Wang et al., 2021) and lake sediments (Wang et al., 2019; Yao et al., 2020) is also important for selecting proper temperature proxies and calibrations for paleotemperature studies. For example, in the case of mixed alkenone production from Group 2 and 3 Isochrysidales, unsaturation ratios of  $C_{38}$  methyl ( $C_{38}$ Me) alkenones may provide more reliable temperature reconstructions than  $U_{37}^{K'}$ , as Group 2 Isochrysidales generally do not produce  $C_{38}$  methyl alkenones (Zheng et al., 2019).

Reconstruction of past Isochrysidales group changes using ancient DNA in sediment cores has been carried out successfully in aquatic systems with anoxic bottom waters and/or in low temperature environments where DNA could be well preserved in sediments of Holocene age (Coolen et al., 2004; D'Andrea et al., 2011). However, relatively poor preservation potential of DNA in ancient sediments presents major

E-mail address: yongsong\_huang@brown.edu (Y. Huang).

<sup>\*</sup> Corresponding author.

challenges to this approach, especially in environments of variable bottom water oxygenation and in warmer environments.

Therefore, examination of characteristics in alkenone/alkenoate profiles represents the most convenient and reliable method to identify alkenone producers. Zheng et al. (2019) summarized the major chemotaxonomic differences in alkenones and alkenoates among the three Isochrysidales groups. These differences include the presence of double bond positional isomers of C37:3Me alkenones in Group 1 alkenones (Dillon et al., 2016), and the lack of production of C38Me and C<sub>39</sub>Et alkenones in Group 2 alkenones which are abundant in Group 3 alkenones. However, demonstration of Group 2 alkenone production in environments with Group 3 alkenones is still challenging, due to the lack of Group 2-specific alkenone or alkenoate biomarkers. We recently demonstrated that C41Me and C42Et alkenones are Group 2-specific biomarkers (Liao et al., 2020). However, the relative abundances of C<sub>41</sub>Me and C<sub>42</sub>Et alkenones can be exceedingly low in certain Group 2 Isochrysidales, making their detection challenging for natural sediment samples.

In this study, we report the first discovery of extended chain length  $C_{37}\text{OEt}$  and  $C_{38}\text{OEt}$  alkenoates in an extensive suite of Group 2 and 3 Isochrysidales culture samples. We performed culture experiments and examined alkenone/alkenoate profiles for multiple species/strains to investigate their production in different groups of Isochrysidales. We also analyzed sediment samples from Lake Van, Lake Fryxell and the Chesapeake Bay to examine the presence/absence of  $C_{37}\text{OEt}$  and  $C_{38}\text{OEt}$  in natural environments. 18S rRNA gene sequencing was performed on one of the Chesapeake Bay sediments to verify the application of  $C_{37}\text{OEt}$  and  $C_{38}\text{OEt}$  alkenoates as chemotaxonomic characters in differentiating different groups of Isochrysidales.

#### 2. Materials and methods

#### 2.1. Culture experiments

The following six Isochrysidales cultured in this study were purchased from various algal culture collections: Group 3 *Gephyrocapsa oceanica* (*G. oceanica*) strains RCC3483 and RCC6484 and Group 2 strain RCC5486 isolated from sea ice (recently classified as Group 2i, Gérikas Ribeiro et al., 2020, Wang et al., 2021) from the Roscoff Culture Collection, Group 3 *Emiliania huxleyi* (*E. huxleyi*) strains NIES1312 and NIES3366 from the National Institute for Environmental Studies, Group 3 *E. huxleyi* strain CCAP920/8 from the Culture Collection of Algae and Protozoa.

Culture growth conditions and harvest procedures followed those reported in Liao et al. (2020). All species/strains were acclimatized for two weeks before the start of corresponding culture experiments with f/2 or k/2 medium (Guillard, 1975). Group 2i strain RCC5486 was cultured at 31 ppt at 6 °C and 15, 21, 26, 31, 38 ppt at 3 °C, *G. oceanica* RCC3483 and RCC6484 at 29 °C, *E. huxleyi* NIES1312 at 9, 12 and 15 °C, NIES3366 at 3, 9 and 15 °C, CCAP920/8 at 3 °C. f/2 medium for RCC5486, NIES1312, NIES3366, CCAP920/8 as well as k/2 medium for RCC3483 and RCC6484 were prepared from seawater collected from Vineyard Sound, Woods Hole, MA, USA at a salinity of 32 ppt (filtered using 0.2  $\mu m$  Whatman nylon membrane filter and then autoclaved). Cultures were grown under a light:dark cycle set at 16:8. The light intensity was 140  $\mu E$  m $^{-2}$  s $^{-1}$  except for *E. huxleyi* NIES1312 and NIES3366 which used a light intensity of 17  $\mu E$  m $^{-2}$  s $^{-1}$ . Cultures experiments were performed in 165 mL medium.

Cultures were harvested at early stationary phase (monitored using hemocytometer counts (Hausser Scientific, PA, USA)) by filtering onto 0.7  $\mu$ m glass fiber filters (Merck Millipore, MA, USA). All filters were wrapped with aluminum foil and immediately frozen at -20 °C for further extraction and analysis (Zheng et al., 2016; Liao et al., 2020).

To obtain additional alkenone/alkenoate profiles from a diversity of Isochrysidales species, we concentrated and re-examined previously characterized culture samples from Group 2 species *Ruttnera lamellosa* 

(R. lamellosa) (CCMP1307), Isochrysis galbana (I. galbana) (CCMP1323), Tisochrysis lutea (T. lutea) (CCMP463), Isochrysis nuda (I. nuda) (RCC1207) and Isochrysis litoralis (I. litoralis) (AC-18) and Group 3 species E. huxleyi (Van556) (Zheng et al., 2019; Liao et al., 2020). Because there is currently no culture of Group 1 Isochrysidales available, surface sediment sample from Lake Braya Sø in Greenland was re-analyzed to represent alkenone profiles for Group 1 species (Longo et al., 2016; Liao et al., 2020).

#### 2.2. Sediment samples

We analyzed alkenone and alkenoate profiles of the following sediment samples: two sediment samples from a 217 m core drilled at hole D of Ahlat Ridge site of Lake Van by the International Continental Drilling Program (ICDP) PALEOVAN project in 2010 (Litt et al., 2012), four surface sediment samples from Chesapeake Bay collected in 2017 and one surface sediment sample from Lake Fryxell collected in 2010 (Supplementary Table S1).

#### 2.3. Analysis of alkenones and alkenoates

Analysis of culture samples and sediment samples followed the procedure reported in Liao et al. (2020). Filters of culture samples were freeze-dried overnight and then sonicated three times with dichloromethane (DCM,  $3\times30$  min, 20 mL each time) for lipid extraction. Sediment samples were extracted using an accelerated solvent extractor (Dionex ASE 200) with dichloromethane/methanol (9:1, v/v). Total extracts of culture samples and sediment samples were divided into three fractions using silica gel (230–400 mesh, 40–63  $\mu m$ ) in glass pipettes and eluted with hexane, DCM and methanol. Alkenones and alkenoates were in the DCM fraction.

DCM fractions (including samples after hydrogenation) were then analyzed by gas chromatography-flame ionization detection (GC-FID, Agilent 7890B) and gas chromatography-electron ionization-mass spectrometry) (GC-MS, Agilent 7890B interfaced to a 5977 Inert Plus MSD) equipped with non-polar HP-1MS columns (30 m  $\times$  250  $\mu$ m  $\times$ 0.25 µm film thickness). 18-Pentatriacontanone was used as an internal standard. For the analysis by GC-FID, the carrier gas was hydrogen. Samples were injected under pulsed splitless mode at 320  $^{\circ}\text{C}.$  The initial pulse pressure was 35 psi for the first 1 min. Then the purge flow to split vent was 35.0 mL/min at 1.1 min. The flow rate (constant flow mode) was 1.5 mL/min. The initial oven temperature was 40 °C for 1 min, then increased to 255 °C at 20 °C/min, then increased to 300 °C at 1 °C/min. then increased to 320  $^{\circ}\text{C}$  at 10  $^{\circ}\text{C/min}$  and held for 30 min. For the analysis by GC-MS, samples were injected under pulsed splitless mode at 320 °C. The initial pulse pressure was 35 psi for the first 0.5 min. The purge flow to split vent was 50 mL/min at 1.1 min. The flow rate (constant flow mode) of helium carrier gas was 1.5 mL/min. The initial oven temperature was 40 °C for 1 min, then increased to 255 °C at 20 °C/ min, then increased to 300  $^{\circ}$ C at 1  $^{\circ}$ C/min, then increased to 320  $^{\circ}$ C at 10 °C/min and held for 30 min. Samples were analyzed under full-scan mode (m/z 50 to 650), selected ion monitoring mode at m/z 88, or at m/z88, 101, 157, 578 and 592. The source temperature was 230  $^{\circ}$ C. The electron ionization energy was 70 eV.

The mid-polarity poly(trifluoropropylmethylsiloxane) column has recently been found to provide much better resolution between alkenoates and alkenones than a non-polar GC column (Zheng et al., 2017). We thus tested the separation performance of our alkenone/alkenoate samples on a GC-FID equipped with a mid-polarity RTX-200 column (105 m  $\times$  250  $\mu m \times$  0.25  $\mu m$  film thickness), following settings reported in Zheng et al. (2017).

#### 2.4. Hydrogenation of alkenones and alkenoates

All culture and sediment samples examined in this work were first analyzed directly using GC-FID (and GC-MS when needed), and

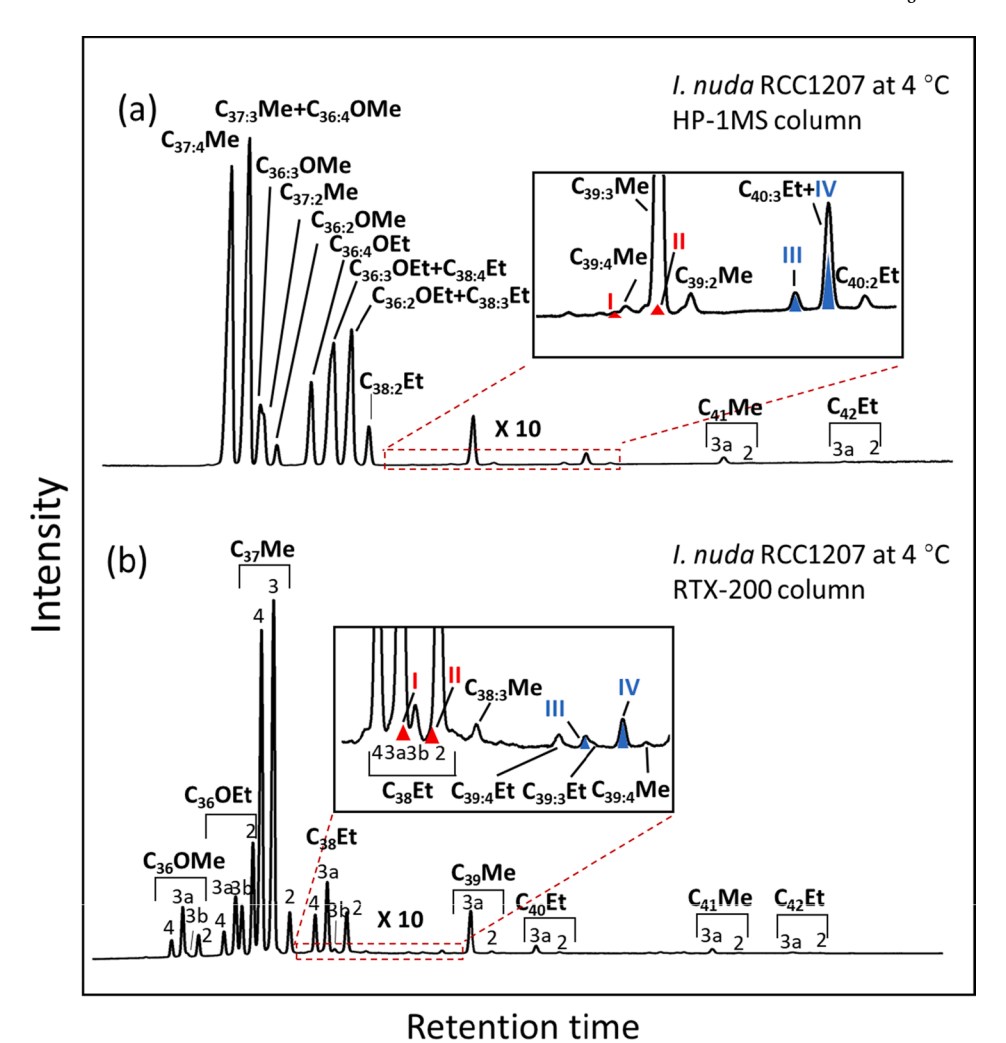


**Fig. 1.** Gas chromatograms showing the distribution of alkenones and alkenoates for *I. nuda* RCC1207 cultured at 4 °C. These analyses were performed with (a) a non-polar HP-1MS column and (b) a mid-polarity RTX-200 column following GC parameters reported previously (Zheng et al., 2017). Compounds I, II, III, IV refer to C<sub>37:3</sub>OEt, C<sub>37:2</sub>OEt, C<sub>38:3</sub>OEt and C<sub>38:2</sub>OEt, respectively.

subsequently hydrogenated. The purpose of hydrogenation is to avoid coelutions and more accurately determine the concentration (and presence or absence) of alkenoates with extended chain lengths (Section 3.3, Supplementary Table S1). For hydrogenation, sample was evaporated to dryness, and then dissolved in acetone solution.  $\sim 7\,$  mg of platinum oxide was added as catalyst. The solution was bubbled with hydrogen gas for 3 h at room temperature. After the reaction finished, the sample was dried and purified with silica gel (230–400 mesh, 40–63  $\mu m$ ) in glass pipettes with hexane, DCM and methanol. Alkenones and alkenoates were in the DCM fraction.

### 2.5. Saponification

To further confirm the existence of the ester group in the newly discovered alkenoates with extended chain lengths, saponification was performed on the hydrogenated sample of *I. nuda* RCC1207 cultured at 10 °C (Supplementary Fig. S3). The disappearance of alkanoates after saponification supports the presence of ester functional groups. For saponification, the sample was evaporated to dryness, and then dissolved in  $\sim 1$  mL of 1 M KOH methanol:water (95:5, v/v) solution. The solution was heated for 3 h at 65 °C. After the sample had cooled to room temperature,  $\sim 1$  mL of 5% (w/v) NaCl solution was added. The solution was then acidified to pH 2 with HCl and extracted with 3  $\times$  1 mL hexane. The sample was finally dried and purified with silica gel (230–400 mesh, 40–63 µm) in glass pipettes with hexane, DCM and methanol. Alkanones

and alkanoates were in the DCM fraction.

#### 2.6. DNA sequencing

We selected one surface sediment sample with surface water salinity at 24.3 ppt (36.99°N, 76.17°W) in Chesapeake Bay for next-generation DNA sequencing, following the same method as described in Wang et al. (2021). In short, the 18S rRNA gene was amplified by adapted versions of Haptophyta-specific primer pair 528Flong and PRYM01 + 7 (F: GCGGTAATTCCAGCTCCAA, R: GATCAGTGAAAACATCCCTGG) (Egge et al., 2013), and sequenced on an Illumina MiSeq using a V2 600-cycle kit (San Diego, CA). Assembled sequences were compiled into different Amplicon Sequence Variants (ASVs) and compared with existing sequences in NCBI GenBank through the Basic Local Alignment Search Tool (https://blast.ncbi.nlm.nih.gov/Blast.cgi). Isochrysidales from surface sediment were archived in NCBI GenBank with accession number MT658506 and MW692054–MW692060.

#### 3. Results and discussion

3.1. GC retention times of di- and tri-unsaturated  $C_{37}\text{OEt}$  and  $C_{38}\text{OEt}$  alkenoates on HP-1MS and RTX-200 columns

No previous studies have revealed the presence of alkenoates with chain lengths longer than C<sub>36</sub>OEt (summarized in Zheng et al., 2019).

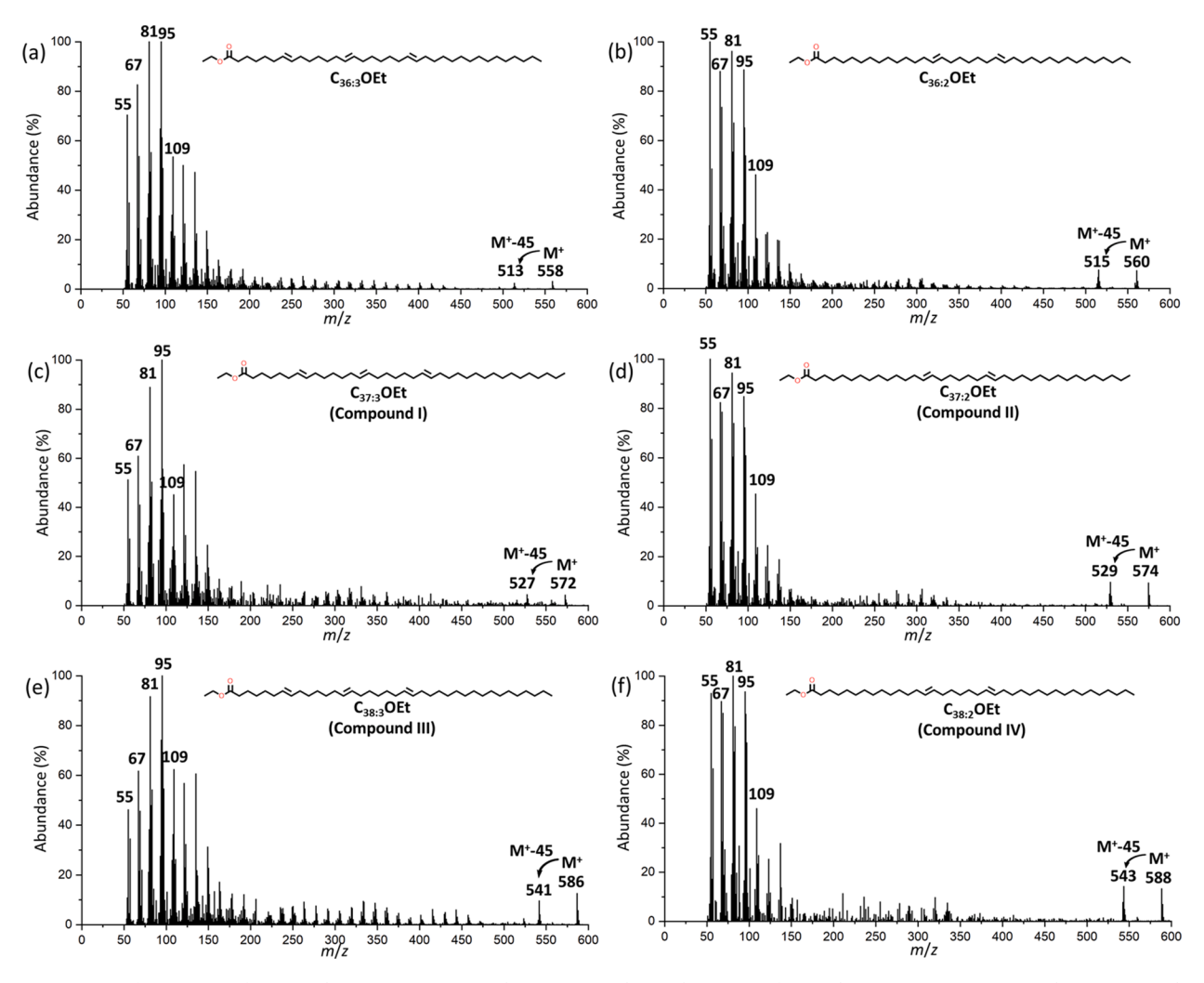


Fig. 2. Mass spectra of (a)  $C_{36:3}$ OEt from *I. nuda* RCC1207 at 4 °C with a RTX-200 column, (b)  $C_{36:2}$ OEt from *T. lutea* CCMP463 at 20 °C with a RTX-200 column, (c)  $C_{37:3}$ OEt from *I. nuda* RCC1207 at 4 °C with an HP-1MS column, (d)  $C_{37:2}$ OEt from *E. huxleyi* CCAP920/8 at 4 °C with a RTX-200 column, (e)  $C_{38:3}$ OEt from *I. nuda* RCC1207 at 4 °C with an HP-1MS column and (f)  $C_{38:2}$ OEt from *T. lutea* CCMP463 at 20 °C with a RTX-200 column. Double bond positions of  $C_{37}$ OEt and  $C_{38}$ OEt are assumed to be the same as  $C_{36}$ OEt (López and Grimalt, 2006; Zheng et al., 2017).

Difficulties in finding these compounds mainly lie in their relatively low concentrations, and extensive co-elutions with C38 to C40 alkenones (Fig. 1). We analyzed our samples using two different GC stationary phases: (1) non-polar poly(dimethylsiloxane) HP-1MS (Fig. 1a) and (2) mid-polarity poly(trifluoropropylmethylsiloxane) RTX-200 (Fig. 1b). Neither GC column can resolve all extended alkenoates from alkenones, but the offset in retention for alkenones and alkenoates between the two columns permits adequate chromatographic resolution for discovering the extended alkenoates. Non-polar HP-1MS column provides complete resolution of C38:3OEt (compound III) from C40Et alkenones and partially resolves C37:3OEt (compound I) from C39Me alkenones. However, co-elutions between C37:2OEt (compound II) and C39:3Me, and between C<sub>38:2</sub>OEt (compound IV) and C<sub>40:3</sub>Et are observed (Fig. 1a). On the other hand, C<sub>37:2</sub>OEt (compound II) and C<sub>38:2</sub>OEt (compound IV) can be partially resolved from alkenones when a mid-polarity RTX-200 column was used (Fig. 1b).

#### 3.2. Mass spectra of extended chain length alkenoates

Obtaining high-quality mass spectra for all four extended chain length alkenoates was challenging. Two different GC columns were used on carefully selected samples to obtain maximal chromatographic resolution and minimize co-elution (Fig. 1). Clean mass spectra for  $C_{37:3}$ OEt (compound I, Fig. 2c) and  $C_{38:3}$ OEt (compound III, Fig. 2e) were

obtained by using the non-polar HP-1MS column on the culture sample of *I. nuda* RCC1207 at 4 °C. Good-quality mass spectra for  $C_{37:2}$ OEt (compound II, Fig. 2d) and  $C_{38:2}$ OEt (compound IV, Fig. 2f) were obtained by using the mid-polarity RTX-200 column on the culture sample of *E. huxleyi* CCAP920/8 at 4 °C and *T. lutea* CCMP463 at 20 °C, respectively.

Mass spectra of  $C_{37}$ OEt and  $C_{38}$ OEt (compounds I to IV) show the same fragmentation patterns as  $C_{36}$ OEt alkenoates (Fig. 2). The mass of molecular ions in  $C_{37:3}$ OEt (compound I, m/z 572, Fig, 2c) and  $C_{38:3}$ OEt (compound III, m/z 586, Fig. 2e) are 14 and 28 amu higher than the ion in  $C_{36:3}$ OEt (m/z 558, Fig. 2a), indicating the additional CH<sub>2</sub> and  $C_{2}$ H<sub>4</sub> groups in these novel compounds. Importantly,  $C_{37}$ OEt and  $C_{38}$ OEt (compound I to IV) feature [M–45]<sup>+</sup> ions, consistent with the fragmentation patterns in  $C_{36:3}$ OEt and  $C_{36:2}$ OEt due to a loss of a CH<sub>3</sub>CH<sub>2</sub>O fragment (Fig. 2a,b).

### 3.3. Mass spectra of hydrogenated alkenoates

Hydrogenation of samples and subsequent analysis with the HP-1MS column allows full resolution of  $C_{37}$  ethyl and  $C_{38}$  ethyl alkanoates from alkanones (Fig. 3a). On the other hand, analysis of hydrogenated sample with the RTX-200 column still shows significant co-elutions (Supplementary Fig. S1). Notably, mass spectra of  $C_{37}$ OEt and  $C_{38}$ OEt alkanoates allow conclusive identifications by comparison of their mass

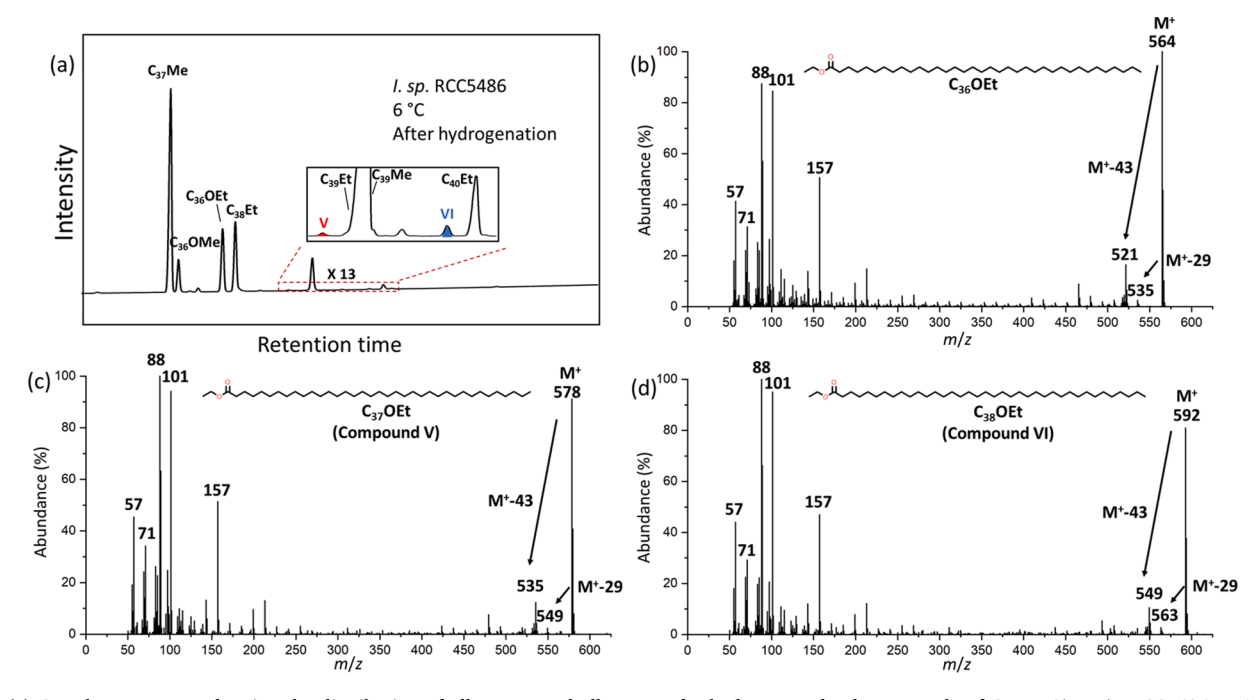
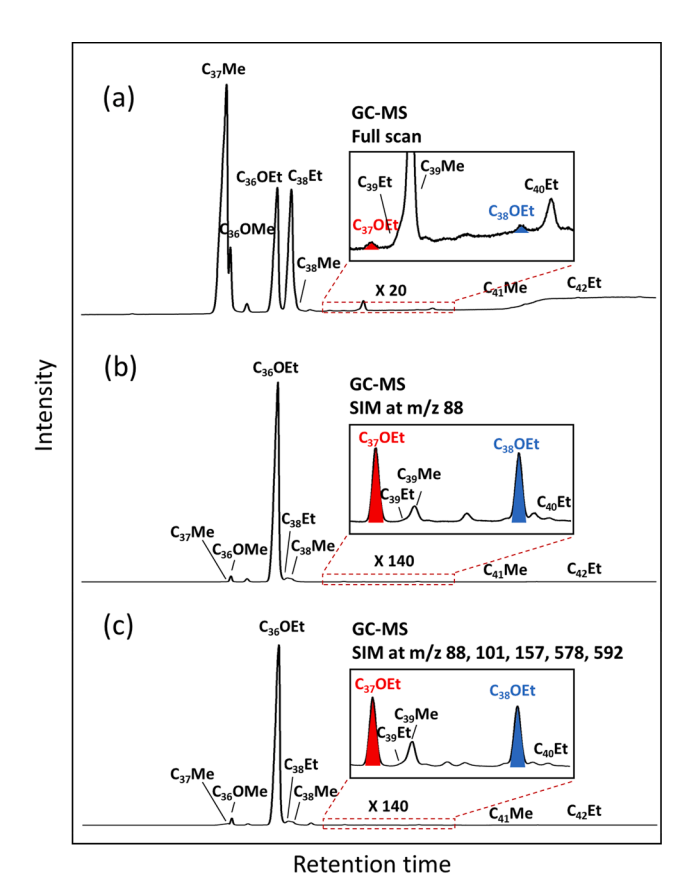


Fig. 3. (a) Gas chromatogram showing the distribution of alkanones and alkanoates for hydrogenated culture sample of Group 2i strain RCC5486 at 6 °C. This analysis was performed on GC-FID equipped with a non-polar HP-1MS column. Mass spectra of hydrogenated  $C_{36}$ OEt (b),  $C_{37}$ OEt (c) and  $C_{38}$ OEt (d) obtained from culture sample of *I. nuda* RCC1207 at 10 °C analyzed with a non-polar HP-1MS column.



**Fig. 4.** Gas chromatograms showing the distribution of alkanones and alkanoates for hydrogenated culture sample of *I. nuda* RCC1207 at 10 °C. These analyses were performed by GC–MS under: (a) full scan mode, (b) selected ion monitoring at m/z 88 and (c) selected ion monitoring at summed m/z 88, 101, 157, 578, 592 with a non-polar HP-1MS GC column.

spectra with shorter chain length homologues (Fig. 3b-d).

After hydrogenation, C<sub>36</sub>OEt, hydrogenated C<sub>37</sub>OEt (compound V) and hydrogenated C<sub>38</sub>OEt (compound VI) all show significant increases of relative intensities for molecular ions (10% before hydrogenation to 93% after hydrogenation on average). These three molecules have ions at  $[M-29]^+$  due to a loss of ethyl group and  $[M-43]^+$  ions due to a loss of propyl fragment (mechanism in Supplementary Fig. S2a). Mass spectra of C36OEt, C37OEt and C38OEt alkanoates contain high abundances of ions at m/z 88 (C<sub>4</sub>H<sub>8</sub>O<sub>2</sub>), 101 (C<sub>5</sub>H<sub>9</sub>O<sub>2</sub>) and 157 (C<sub>9</sub>H<sub>17</sub>O<sub>2</sub>), which are characteristic for ethyl esters (Sun and Holman, 1968). Ions at m/z 88 are produced through McLafferty rearrangement (Supplementary Fig. S2b). Generation of ions at m/z 101 and m/z 157 involves a corresponding hydrogen shift process (Supplementary Fig. S2c,d). The existence of an ester group in the hydrogenated C<sub>37</sub>OEt (compound V) and C38OEt (compound VI) alkanoates was further evidenced by the removal of these compounds after saponification (Supplementary Fig. S3).

# 3.4. Detection of $C_{37}$ OEt and $C_{38}$ OEt alkanoates with GC–MS selected ion monitoring

Mass spectra of hydrogenated  $C_{37}$ OEt and  $C_{38}$ OEt alkanoates contain high abundances of rare fragment ions related to the ester group (m/z 88, 101, 157) and molecular ion peaks (m/z 578 for  $C_{37}$ OEt and 592 for  $C_{38}$ OEt). This allows detection under selected ion monitoring mode to increase the detection limit and sensitivity. Especially, the even mass ion at m/z 88 caused by McLafferty rearrangement is characteristic for ethyl esters but generally small or absent in mass spectra of other molecules in natural products. Selected ion monitoring of m/z 88 greatly reduces the relative peak areas for alkanones and decreases the detection limit of ethyl esters to 8.8 pg (Fig. 4b). In comparison, the detection limit was 570 pg for ethyl esters under full scan mode (Fig. 4a). The addition of more characteristic ions related to the ester group (m/z 101, 157) and molecular ion peaks (m/z 578 for  $C_{37}$ OEt and 592 for  $C_{38}$ OEt) further decreases the detection limit to 6.1 pg, but also with more non-target peaks shown in the mass chromatogram (Fig. 4c).

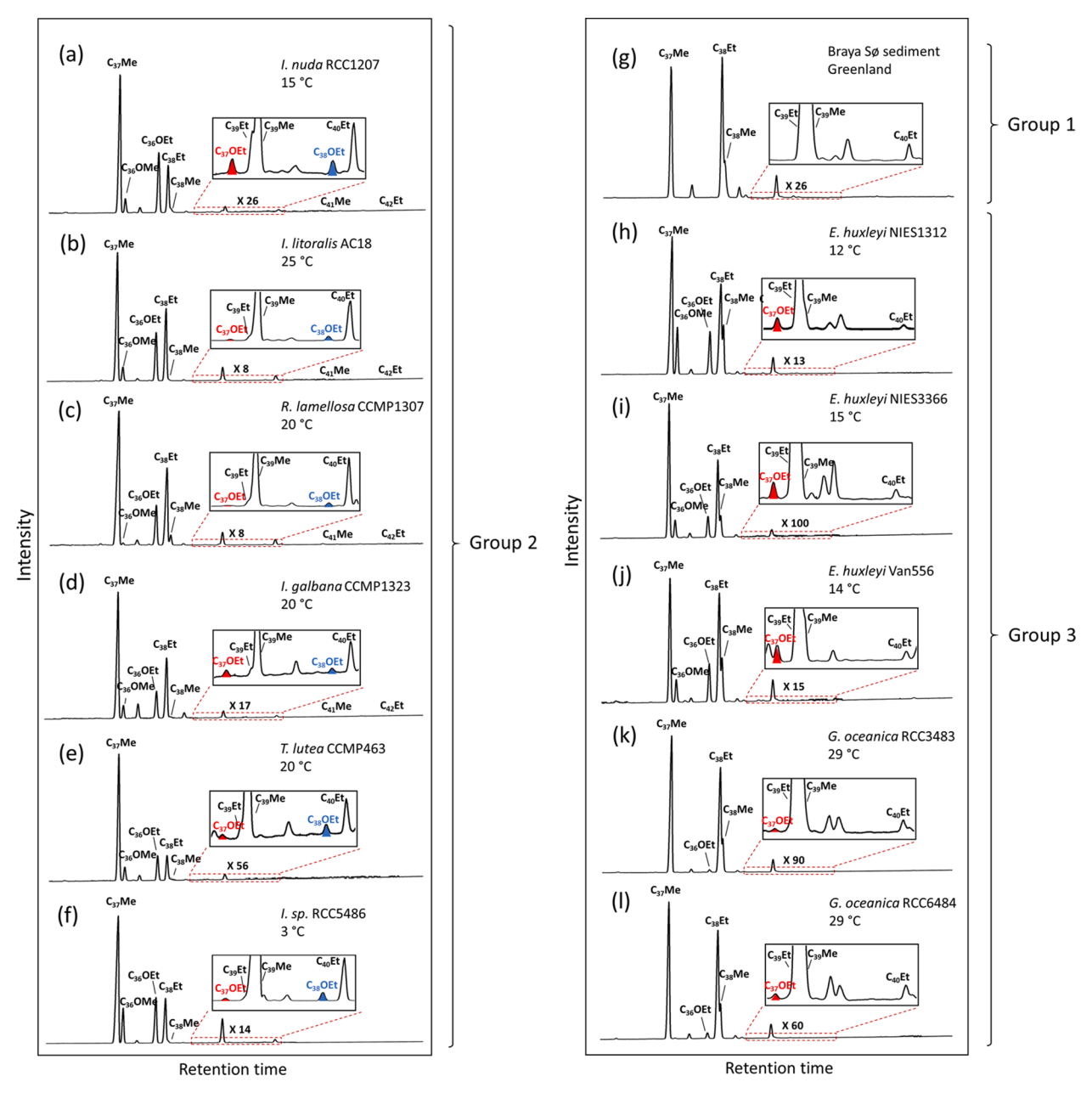


Fig. 5. Gas chromatograms showing the distribution of alkanones and alkanoates for different groups of Isochrysidales after hydrogenation. Group 2 samples include; (a) culture samples of *I. nuda* RCC1207, (b) *I. litoralis* AC18, (c) *R. lamellosa* CCMP1307, (d) *I. galbana* CCMP1323, (e) *T. lutea* CCMP463 and (f) Group 2i *I. sp.* RCC5486. (g) Lake Braya Sø sediment sample shows representative alkenone profiles for Group 1 species. Group 3 samples include culture samples of: (h) *E. huxleyi* NIES1312, (i) *E. huxleyi* NIES3366, (j) *E. huxleyi* Van556, (k) *G. oceanica* RCC3483 and (l) *G. oceanica* RCC6484. These analyses were performed on GC-FID equipped with a non-polar HP-1MS column.

# 3.5. $C_{37}$ OEt and $C_{38}$ OEt alkenoates as biomarkers for different groups of Isochrysidales

Different groups of Isochrysidales differ in the production of  $C_{37}OEt$  and  $C_{38}OEt$  alkenoates. Group 1 Isochrysidales do not produce alkenoates (Fig. 5g; Zheng et al., 2019). The  $C_{37}OEt$  alkenoate was found in culture samples of both Group 2 (*I. nuda, I. litoralis, R. lamellosa, I. galbana, T. lutea* and one Group 2i strain, Fig. 5a–f) and Group 3 (*E. huxleyi* and *G. oceanica*, Fig. 5h–l) Isochrysidales. Among Group 2 Isochrysidales, *I. galbana* has the highest ratio of  $C_{37}OEt/C_{37}Me$  (0.53%), with the lowest ratio in *R. lamellosa* (0.04%).  $C_{37}OEt/C_{37}Me$  ratios of Group 3 E. huxleyi (0.82%) are on average 17 times higher than those of *G. oceanica* (0.05%) (Supplementary Fig. S4a). Notably, different strains of *E. huxleyi* also vary on the ratios of  $C_{37}OEt/C_{37}Me$ :

*E. huxleyi* Van556 shows the highest ratio (1.37%), followed by *E. huxleyi* NIES1312 (0.90%) and lowest ratio in *E. huxleyi* NIES3366 (0.21%).  $C_{38}$ OEt alkenoates were only found in samples of Group 2 Isochrysidales, with the highest  $C_{38}$ OEt/ $C_{37}$ Me ratio in *R. lamellosa* (0.87%) and lowest ratio in *T. lutea* (0.08%) (Supplementary Fig. S4b). Collectively, our data suggest that the presence/absence of  $C_{37}$ OEt and  $C_{38}$ OEt permits differentiation among three groups of Isochrysidales: no alkenoates in Group 1 species, only  $C_{37}$ OEt in Group 3 species and both  $C_{37}$ OEt and  $C_{38}$ OEt in Group 2 species.  $C_{38}$ OEt alkenoates could thus be used as biomarkers to identify the alkenone/alkenoate contribution from Group 2 Isochrysidales in settings where Group 1 and 2 mix (e.g., Yao et al., 2020), and Group 2 and 3 mix (e.g., Kaiser et al., 2019; Huang et al., 2021).

Among three groups of Isochrysidales, only Group 2 Isochrysidales

produce extended chain length alkenones ( $C_{41}$ Me and  $C_{42}$ Et) (Liao et al., 2020) and alkenoates ( $C_{38}$ OEt) (Supplementary Fig. S5b), but generally do not produce  $C_{38}$ Me and  $C_{39}$ Et alkenones that are abundant in both Group 1 and Group 3 Isochrysidales (Supplementary Fig. S5a,c). Thus, production of extended chain length alkenones and alkenoates in Group 2 species may help compensate for their lack of shorter-chain  $C_{38}$ Me and  $C_{39}$ Et alkenones (Liao et al., 2020).

Alkenoates are thought to be more susceptible to diagenetic degradation than alkenones (Grimalt et al., 2000). For example, Teece et al. (1998) show that alkenoates degrade preferentially relative to alkenones in anaerobic conditions during a laboratory simulation experiment. However, alkenoates were found, along with alkenones, in 6-millionyear-old sediments from the Japan Trench (Brassell et al., 1980; Marlowe et al., 1984), indicating that alkenoates are also diagenetically fairly stable biomarkers. Alkenoates are rarely reported in previous studies, mainly because during the sample processing, sediment extracts are often saponified to remove alkenoates to avoid coelutions and to obtain a more accurate measure of alkenone unsaturation indices (e.g., Müller et al., 1998; Randlett et al., 2014). However, when mid-polarity GC columns are used (Longo et al., 2013), major alkenones and alkenoates are well separated from each other hence saponification may no longer be necessary. A combined study of both alkenones and alkenoates can thus provide important information regarding production from different groups of Isochrysidales in natural samples.

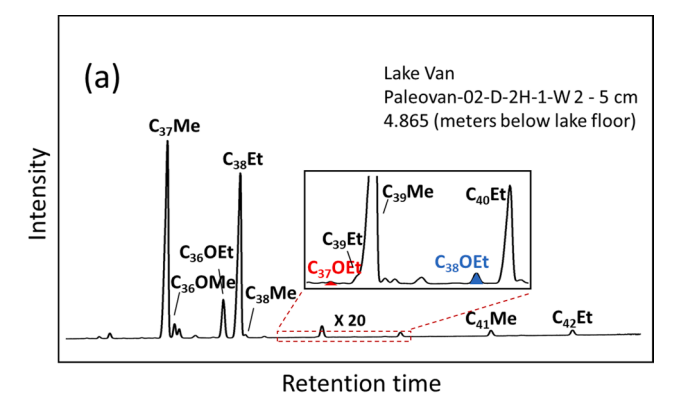
# 3.6. Influence of salinity and temperature on the production of $C_{37}$ OEt and $C_{38}$ OEt alkenoates

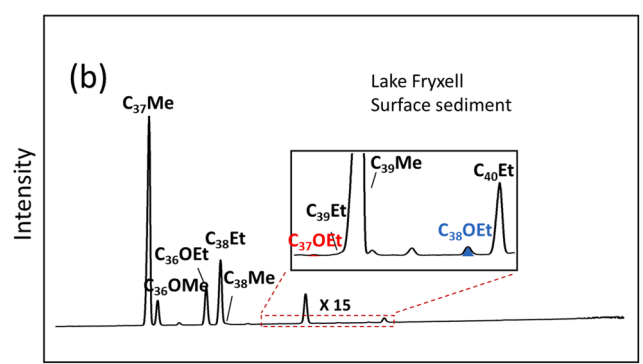
We performed preliminary experiments to investigate the influence of salinity on the production of  $C_{37}$ OEt and  $C_{38}$ OEt for the Group 2i strain RCC5486. For both  $C_{37}$ OEt and  $C_{38}$ OEt alkenoates, we observed a decreasing  $C_{37}$ OEt and  $C_{38}$ OEt ratio relative to  $C_{37}$ Me alkenones at higher salinities. From 15 to 38 ppt,  $C_{37}$ OEt/ $C_{37}$ Me ratio decreases by 44% and  $C_{38}$ OEt/ $C_{37}$ Me ratio decreases by 38% (Supplementary Fig. S6). However, a salinity change from 15 to 38 ppt had no significant influence on the growth rates for the Group 2i strain RCC5486 (Supplementary Fig. S7). This suggests changes in  $C_{37}$ OEt/ $C_{37}$ Me or  $C_{38}$ OEt/ $C_{37}$ Me ratios may not be caused by growth rate changes at different salinity levels. More study is needed to understand the factors controlling the changes in the  $C_{37}$ OEt/ $C_{37}$ Me or  $C_{38}$ OEt/ $C_{37}$ Me ratios at different salinity.

The influence of temperature on the production of C<sub>37</sub>OEt and C<sub>38</sub>OEt varies among different species/strains. For all strains of Group 3 E. huxleyi (NIES1312, NIES3366, Van556), ratios of C<sub>37</sub>OEt alkenoates relative to C<sub>37</sub>Me alkenones decrease with increasing temperatures, similar to the trend of C<sub>36</sub>OEt and C<sub>36</sub>OMe alkenoates as reported previously in cultures of E. huxleyi and G. oceanica (Conte et al., 1998) and ocean suspended particulate matter samples (Conte and Eglinton, 1993). For Group 2 species, however, we didn't observe an obvious correlation between temperature and ratios of C<sub>37</sub>OEt relative to C<sub>37</sub>Me. On the other hand, ratios of C38OEt/C37Me increase with increasing temperatures for I. nuda, but with decreasing temperatures for I. galbana. No obvious correlation was found between C38OEt ratios and temperatures for T. lutea, R. lamellosa and I. litoralis. Different correlations between alkenoate ratios and temperatures among Group 2 species were also found for C36OEt and C36OMe alkenoates (e.g., with increasing temperature, I. nuda and I. litoralis have higher ratios of C<sub>36</sub>OEt/C<sub>37</sub>Me while I. galbana and T. lutea have lower ratios of C36OEt/C37Me).

# 3.7. Detection of $C_{38}$ OEt in sediment samples and comparison with DNA data

We selected sediment samples containing demonstrated Group 2 Isochrysidales, in order to validate the extended chain length  $C_{38}OEt$  alkenoates as Group 2 biomarkers. These samples included four surface sediments from Chesapeake Bay, one sample from Lake Fryxell and two





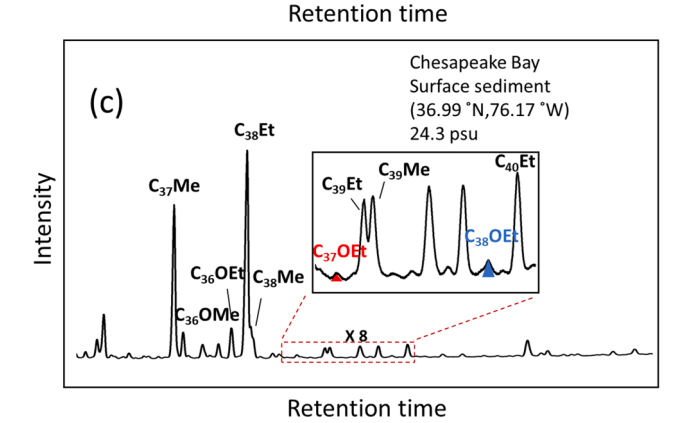


**Fig. 6.** Gas chromatograms showing the distribution of alkanones and alkanoates for hydrogenated downcore sample from: (a) Lake Van at 4.865 m below lake floor (mblf), (b) surface sample from Lake Fryxell and (c) surface sample from Chesapeake Bay. Presence or absence of  $C_{37}$ OEt and  $C_{38}$ OEt was determined using selected ion monitoring mode at m/z 88 with a non-polar HP-1MS column (Supplementary Fig. S8).

downcore samples from Lake Van. Lake Van and Lake Fryxell have been previously examined for 18S rRNA in sediment and/or water column samples. In both Lake Van and Lake Fryxell, only sequences of Group 2 Isochrysidales were recovered (Jaraula et al., 2010; Randlett et al., 2014). We carried out additional next-generation DNA sequencing on one of the Chesapeake Bay sediments with the highest surface water salinity (24.3 ppt). We identified eight Amplicon Sequence Variants (ASVs) (Supplementary Table S2). Four ASVs detected shared 99.44% to 100% identity with I. galbana CCAP 949/1. The remaining ASVs shared 99.72 to 100% identity with E. huxleyi RCC6856. This suggests a mixed alkenone/alkenoate production from Group 2 and 3 Isochrysidales in this Chesapeake Bay sample. The surface water salinity of other Chesapeake Bay samples ranges from 15.4 to 16.8 ppt (Supplementary Table S1). Based on distribution characteristics of Isochrysidales in the Baltic Sea (Kaiser et al., 2019), Group 2 species should also contribute to the production of alkenones and alkenoates in these Chesapeake Bay samples within this salinity range.

Analysis of alkenone and alkenoate profiles in sediments is consistent with DNA sequencing results: we identified C38OEt alkenoates in all sediment samples examined (Fig. 6, Supplementary Table S1). Lake Fryxell surface sediment has 0.31% C<sub>38</sub>OEt/C<sub>37</sub>Me. Lake Van samples on average have 0.42% C<sub>38</sub>OEt/C<sub>37</sub>Me. The Chesapeake Bay samples on average have 1.88% C<sub>38</sub>OEt/C<sub>37</sub>Me. On the other hand, C<sub>37</sub>OEt was identified in nearly all sediments except two samples from Chesapeake Bay due to their low alkenone/alkenoate concentrations (Supplementary Table S1). In the Chesapeake Bay sample containing DNA sequences of both Group 2 and Group 3 Isochrysidales (Fig. 6c), mixed production by Group 2 and Group 3 Isochrysidales can be readily identified based on alkenone and alkenoate profiles. The presence of  $C_{38}OEt$  (0.35% relative to C<sub>37</sub>Me) suggests production from Group 2 Isochrysidales. The contribution from Group 3 Isochrysidales can be determined based on the relatively high ratios of C38Me and C39Et over C37Me alkenones (Supplementary Fig. S5, Supplementary Table S1). Collectively, our data from culture samples and sediment samples suggest C38OEt is a robust biomarker for identifying the Group 2 contributions in saline lakes and estuaries.

#### 4. Conclusions

We report the first discovery and structure identification of extended chain length C<sub>37</sub>OEt and C<sub>38</sub>OEt alkenoates in Group 2 and/or Group 3 Isochrysidales based on extensive culture samples. Importantly, these extended chain length alkenoates can serve as specific biomarkers to differentiate inputs from all three groups of Isochrysidales: Group 1 species do not produce alkenoates, Group 2 species produce both C<sub>37</sub>OEt and C<sub>38</sub>OEt, and Group 3 species only produce C<sub>37</sub>OEt. Therefore, C38OEt alkenoates are specific biomarkers for Group 2 Isochrysidales. The application of C<sub>38</sub>OEt as Group 2 biomarkers is further confirmed by its presence in sediment samples from Lake Fryxell, Lake Van and Chesapeake Bay where sequences of Group 2 DNA have been recovered. GC-MS detection sensitivity of extended alkenoates in sediment samples can be greatly enhanced under selected ion monitoring mode using characteristic McLafferty rearrangement ion at m/z 88, or summed m/z88, 101, 157, 578 and 592 fragment ions on hydrogenated ketone/ester fractions.

### **Declaration of Competing Interest**

The authors declare that they have no known competing financial interests or personal relationships that could have appeared to influence the work reported in this paper.

### Acknowledgments

This work was supported by the United States National Science Foundation awards to Y.H. (EAR-1762431). We would like to thank Tyler Kartzinel, Fred Jackson, Nicholas Vasques and Sophia Yin for their assistance during the culture growth experiments. We are also grateful for the comments from two anonymous reviewers, which helped us improve the manuscript.

#### Appendix A. Supplementary material

Supplementary data to this article can be found online at https://doi.org/10.1016/j.orggeochem.2021.104303.

#### References

Araie, H., Nakamura, H., Toney, J.L., Haig, H.A., Plancq, J., Shiratori, T., Leavitt, P.R., Seki, O., Ishida, K.-I., Sawada, K., Suzuki, I., Shiraiwa, Y., 2018. Novel alkenone-producing strains of genus Isochrysis (Haptophyta) isolated from Canadian saline lakes show temperature sensitivity of alkenones and alkenoates. Organic Geochemistry 121, 89–103.

- Brassell, S.C., Comet, P.A., Eglinton, G., Isaacson, P.J., McEvoy, J., Maxwell, J.R., Thompson, I.D., Tibbetts, P.J.C., Volkman, J.K., 1980. Preliminary lipid analyses of sections 440A-7-6, 440B-3-5, 440B-8-4, 440B-68-2, and 436-11-4: Legs 56 and 57, Deep Sea Drilling Project. Initial Reports of the Deep Sea Drilling Project 56-57, 1367-1390.
- Brassell, S.C., Eglinton, G., Marlowe, I.T., Pflaumann, U., Sarnthein, M., 1986. Molecular stratigraphy: a new tool for climatic assessment. Nature 320, 129–133.
- Conte, M.H., Eglinton, G., 1993. Alkenone and alkenoate distributions within the euphotic zone of the eastern North Atlantic: correlation with production temperature. Deep Sea Research Part I: Oceanographic Research Papers 40, 1935–1961.
- Conte, M.H., Thompson, A., Lesley, D., Harris, R.P., 1998. Genetic and physiological influences on the alkenone/alkenoate versus growth temperature relationship in *Emiliania huxleyi* and *Gephyrocapsa oceanica*. Geochimica et Cosmochimica Acta 62, 51–68.
- Coolen, M.J.L., Muyzer, G., Rijpstra, W.I.C., Schouten, S., Volkman, J.K., Sinninghe Damsté, S., 2004. Combined DNA and lipid analyses of sediments reveal changes in Holocene haptophyte and diatom populations in an Antarctic lake. Earth and Planetary Science Letters 223, 225–239.
- D'Andrea, W.J., Huang, Y., Fritz, S.C., Anderson, N.J., 2011. Abrupt Holocene climate change as an important factor for human migration in West Greenland. Proceedings of the National Academy of Sciences 108, 9765–9769.
- Dillon, J.T., Longo, W.M., Zhang, Y., Torozo, R., Huang, Y., 2016. Identification of double-bond positions in isomeric alkenones from a lacustrine haptophyte. Rapid Communications in Mass Spectrometry 30, 112–118.
- Egge, E., Bittner, L., Andersen, T., Audic, S., de Vargas, C., Edvardsen, B., Lin, S., 2013. 454 pyrosequencing to describe microbial eukaryotic community composition, diversity and relative abundance: a test for marine haptophytes. PLoS ONE 8, e74371.
- Gérikas Ribeiro, C., Dos Santos, A.L., Gourvil, P., Le Gall, F., Marie, D., Tragin, M., Probert, I., Vaulot, D., Michel, C., 2020. Culturable diversity of Arctic phytoplankton during pack ice melting. Elementa: Science of the Anthropocene 8.
- Grimalt, J.O., Rullkötter, J., Sicre, M.-A., Summons, R., Farrington, J., Harvey, H.R., Goñi, M., Sawada, K., 2000. Modifications of the C<sub>37</sub> alkenone and alkenoate composition in the water column and sediment: Possible implications for sea surface temperature estimates in paleoceanography. Geochemistry, Geophysics, Geosystems 1, 2000GC000053.
- Guillard, R.R.L., 1975. Culture of phytoplankton for feeding marine invertebrates. In: Smith, W.L., Chanley, M.H. (Eds.), Culture of Marine Invertebrate Animals. Plenum Press, New York, USA, pp. 26–60.
- Huang, Y., Zheng, Y., Heng, P., Giosan, L., Coolen, M.J.L., 2021. Black Sea paleosalinity evolution since the last deglaciation reconstructed from alkenone-inferred Isochrysidales diversity. Earth and Planetary Science Letters 564, 116881.
- Jaraula, C.M.B., Brassell, S.C., Morgan-Kiss, R.M., Doran, P.T., Kenig, F., 2010. Origin and tentative identification of tri to pentaunsaturated ketones in sediments from Lake Fryxell, East Antarctica. Organic Geochemistry 41, 386–397.
- Kaiser, J., Wang, K.J., Rott, D., Li, G., Zheng, Y., Amaral-Zettler, L., Arz, H.W., Huang, Y., 2019. Changes in long chain alkenone distributions and Isochrysidales groups along the Baltic Sea salinity gradient. Organic Geochemistry 127, 92–103.
  Liao, S., Yao, Y., Wang, L.i., Wang, K.J., Amaral-Zettler, L., Longo, W.M., Huang, Y.,
- Liao, S., Yao, Y., Wang, L.i., Wang, K.J., Amaral-Zettler, L., Longo, W.M., Huang, Y., 2020. C<sub>41</sub> methyl and C<sub>42</sub> ethyl alkenones are biomarkers for Group II Isochrysidales. Organic Geochemistry 147, 104081.
- Litt, T., Anselmetti, F.S., Baumgarten, H., Beer, J., Cagatay, N., Cukur, D., Damci, E., Glombitza, C., Haug, G., Heumann, G., 2012. 500,000 Years of environmental history in eastern Anatolia: the PALEOVAN drilling project. Scientific Drilling 14, 18–29.
- Longo, W.M., Dillon, J.T., Tarozo, R., Salacup, J.M., Huang, Y., 2013. Unprecedented separation of long chain alkenones from gas chromatography with a poly (trifluoropropylmethylsiloxane) stationary phase. Organic Geochemistry 65, 94–102
- Longo, W.M., Theroux, S., Giblin, A.E., Zheng, Y., Dillon, J.T., Huang, Y., 2016. Temperature calibration and phylogenetically distinct distributions for freshwater alkenones: Evidence from northern Alaskan lakes. Geochimica et Cosmochimica Acta 180, 177–196.
- Longo, W.M., Huang, Y., Yao, Y., Zhao, J., Giblin, A.E., Wang, X., Zech, R., Haberzettl, T.,
   Jardillier, L., Toney, J., Liu, Z., Krivonogov, S., Kolpakova, M., Chu, G., D'Andrea, W.
   J., Harada, N., Nagashima, K., Sato, M., Yonenobu, H., Yamada, K., Gotanda, K.,
   Shinozuka, Y., 2018. Widespread occurrence of distinct alkenones from Group I
   haptophytes in freshwater lakes: Implications for paleotemperature and
   paleoenvironmental reconstructions. Earth and Planetary Science Letters 492,
   239–250
- López, J.F., Grimalt, J.O., 2006. Reassessment of the structural composition of the alkenone distributions in natural environments using an improved method for double bond location based on GC-MS analysis of cyclopropylimines. Journal of the American Society for Mass Spectrometry 17, 710–720.
- Marlowe, I.T., Brassell, S.C., Eglinton, G., Green, J.C., 1984. Long chain unsaturated ketones and esters in living algae and marine sediments. Organic Geochemistry 6, 135–141.
- Müller, P.J., Kirst, G., Ruhland, G., von Storch, I., Rosell-Melé, A., 1998. Calibration of the alkenone paleotemperature index U37K' based on core-tops from the eastern South Atlantic and the global ocean (60°N–60°S). Geochimica et Cosmochimica Acta 62, 1757–1772.
- Randlett, M.E., Coolen, M.J.L., Stockhecke, M., Pickarski, N., Litt, T., Balkema, C., Kwiecien, O., Tomonaga, Y., Wehrli, B., Schubert, C.J., 2014. Alkenone distribution in Lake Van sediment over the last 270 ka: influence of temperature and haptophyte species composition. Ouaternary Science Reviews 104, 53–62.

- Rosell-Melé, A., Comes, P., 1999. Evidence for a warm Last Glacial Maximum in the Nordic seas or an example of shortcomings in  $U_{37}^{\ \ K}$  and  $U_{37}^{\ \ K}$  to estimate low sea surface temperature? Paleoceanography 14, 770–776.
- Sun, K.K., Holman, R.T., 1968. Mass spectrometry of lipid molecules. Journal of the American Oil Chemists' Society 45, 810–817.
- Teece, M.A., Getliff, J.M., Leftley, J.W., Parkes, R.J., Maxwell, J.R., 1998. Microbial degradation of the marine prymnesiophyte *Emiliania huxleyi* under oxic and anoxic conditions as a model for early diagenesis: long chain alkadienes, alkenones and alkyl alkenoates. Organic Geochemistry 29, 863–880.
- Theroux, S., D'Andrea, W.J., Toney, J., Amaral-Zettler, L., Huang, Y., 2010. Phylogenetic diversity and evolutionary relatedness of alkenone-producing haptophyte algae in lakes: Implications for continental paleotemperature reconstructions. Earth and Planetary Science Letters 300, 311–320.
- Theroux, S., Huang, Y., Toney, J.L., Andersen, R., Nyren, P., Bohn, R., Salacup, J., Murphy, L., Amaral-Zettler, L., 2020. Successional blooms of alkenone-producing haptophytes in Lake George, North Dakota: Implications for continental paleoclimate reconstructions. Limnology and Oceanography 65, 413–425.
- Tzanova, A., Herbert, T.D., 2015. Regional and global significance of Pliocene sea surface temperatures from the Gulf of Cadiz (Site U1387) and the Mediterranean. Global and Planetary Change 133, 371–377.

- Wang, K.J., O'Donnell, J.A., Longo, W.M., Amaral-Zettler, L., Li, G., Yao, Y., Huang, Y., 2019. Group I alkenones and Isochrysidales in the world's largest maar lakes and their potential paleoclimate applications. Organic Geochemistry 138, 103924.
- Wang, K.J., Huang, Y., Majaneva, M., Belt, S.T., Liao, S., Novak, J., Kartzinel, T.R., Herbert, T.D., Richter, N., Cabedo-Sanz, P., 2021. Group 2i Isochrysidales produce characteristic alkenones reflecting sea ice distribution. Nature Communications 12, 1–10.
- Yao, Y., Lan, J., Zhao, J., Vachula, R.S., Xu, H., Cai, Y., Cheng, H., Huang, Y., 2020. Abrupt freshening since the early Little Ice Age in Lake Sayram of arid central Asia inferred from an alkenone isomer proxy. Geophysical Research Letters 47, e2020GL089257.
- Zheng, Y., Huang, Y., Andersen, R.A., Amaral-Zettler, L.A., 2016. Excluding the diunsaturated alkenone in the U37K index strengthens temperature correlation for the common lacustrine and brackish-water haptophytes. Geochimica et Cosmochimica Acta 175, 36–46.
- Zheng, Y., Tarozo, R., Huang, Y., 2017. Optimizing chromatographic resolution for simultaneous quantification of long chain alkenones, alkenoates and their double bond positional isomers. Organic Geochemistry 111, 136–143.
- Zheng, Y., Heng, P., Conte, M.H., Vachula, R.S., Huang, Y., 2019. Systematic chemotaxonomic profiling and novel paleotemperature indices based on alkenones and alkenoates: Potential for disentangling mixed species input. Organic Geochemistry 128, 26–41.